OPTIMIZATION OF SnO2 THIN FILMS FOR LOW TEMPERATURE NO2 SENSORS APPLICATIONS

Antonio Assaf, Mohammed Zeghouane, Jean-Raoul Plaussu, Sebastien Cavalaglio, Bernard Pelissier, Franck Bassani, Ingrid Canero-Infante, Tomas Fiorido, Marc Bendahan, Stephane Monfray, et al.

OPTIMIZATION OF SnO_2 THIN FILMS FOR LOW TEMPERATURE NO_2 SENSORS APPLICATIONS.

Antonio Assaf [a,b], Mohammed Zeghouane[b], Jean-Raoul Plaussu[b], Sebastien Cavalaglio[b], Bernard Pelissier[b], Franck Bassani[b], Ingrid Canero-Infante[a], Tomas Fiorido[c], Marc Bendahan[c], Stephane Monfray [d], Bassem Salem[b], Bertrand Vilquin[a], Abdelkader Souifi[a,b].

a. Université de Lyon, CNRS, INSA Lyon, Ecole Centrale de Lyon, UCBL, INL, UMR 5270, Villeurbanne, France
b. Univ. Grenoble Alpes, CNRS, CEA/ LETI Minatec, Grenoble INP, LTM, UMR 5129 Grenoble, France
c. Aix Marseille Univ, Université de Toulon, CNRS, IM2NP, UMR 7334, Marseille, France
d. STMicroelectronics, 850 Rue Jean Monnet, 38920 Crolles, France

* Email: antonio.assaf@insa-lyon.fr

Abstract

In this work, a high-performance n-type semiconductor gas sensor based on undoped-SnO_2 thin films deposited by conventional radio-frequency (RF) – magnetron sputtering process was successfully fabricated. The structure, morphology, and chemical composition of the sensing material were investigated using X-ray diffraction (XRD), Atomic Force Microscopy (AFM) and X-ray photoelectron spectroscopy (XPS) respectively. The end results show that the thin film has a poly-crystalline structure with the presence of oxygen vacancies. The resistive sensor architecture has been simulated using TCAD SILVACO software's in order to optimize the geometry for a sensor response optimization.

In this study, undoped-SnO_2 resistive gas sensor exhibits compelling sensing performance for detecting 3 ppm of NO_2 mixed with dry air at low operating temperature, around 100°C. 3 ppm represents the maximum level of NO_2 concentration beyond which short-term exposure presents a risk to human health or environmental degradation. Lower concentrations were also investigated in our study and the lowest NO_2 concentration evaluated is about 0.25 ppm.

Keywords: Undoped-SnO_2 gas sensors, TCAD simulations, low operating temperature, NO_2 sensing.

1. INTRODUCTION

NO_2 is one of the largest automobile pollutants and presents harmful effects on environment (acid rain) and health effects on humans [1]. In this context, several studies have been conducted in order to develop microsensors for air quality monitoring. As a result, an exponential increase of the gas sensors market is observed in recent years [2].

In the context of the Internet of Things (IoT) and the high demand for real-time measurements, autonomous sensors present a real advantage. Lowering the operating temperature of the sensor is one of the solutions to reduce the power consumption for a better autonomy. The working temperature of a conventional sputtered metal oxide gas sensor varies between 200-300°C for NO_2 sensing applications [3,4]. The main objective of our work is to study undopped-SnO_2 in order to lower the operating temperature of NO_2 sensors.

2 Simulation and experimental setup

2.1 Simulating the sensor

The main purpose of the simulation is to study carefully the effect of geometrical parameters on the electric properties of the sensor. The objective is to obtain a well-defined geometry to achieve good sensing performance. The sensor (inter-digitated electrodes + SnO_2 film) is simulated using SILVACO TCAD tools. The simulation is carried out with 3D layout. Figure 1 displays the sensor scheme from two angles, top view and cross section. The materials used for the electrodes are titanium and platinum with a total thickness of 45 nm. The number, length and width of electrodes fingers are indicated in figure 1. Different values of the gap (g) between electrodes were examined. The chosen g values are: 5, 10 and 20 μm.

The SnO_2 film is divided into two layers: the top layer, which represents the surface of the film, and the bottom layer, representing the bulk. These layers are represented in two different colors (in light and dark green, respectively) in figure 1b.

To understand the difference between these two SnO_2 layers, we give a brief summary on the mechanism of a resistive gas sensor [5]. When gas molecules are adsorbed on the surface of a SnO_2 film, an exchange of electrons takes place between the film surface and the gas molecules. However, the concentration of the free electrons varies during the gas detection.

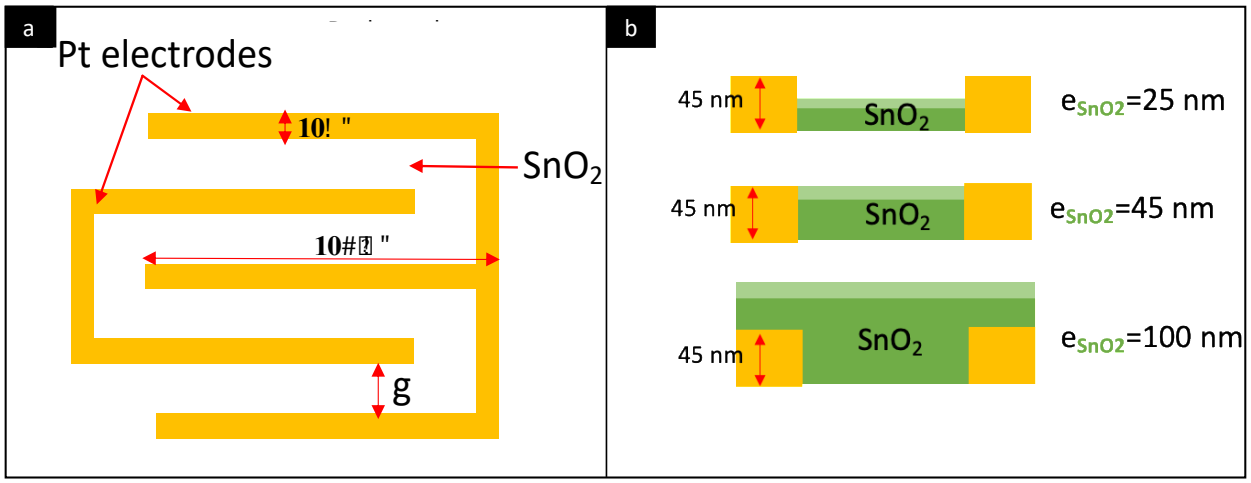

Figure 1:Top view of the simulated sensor b) cross section of the simulated sensor with variable SnO_2 thickness. The geometrical parameter given on the schemes.

Since SnO_2 is not included in the SILVACO material library, we have used silicon, and adjust the material parameters, in a way to introduce the SnO_2 electric properties. Moreover, a n-type doping is introduced in the material in order to consider the different electron density in the top and bottom layers. The number of dopants, N_2, of the top layer, varies under two conditions: $N_2 = N_1$ (N_1 being the number of dopants of the bottom layer) when the sensor is exposed to the air, whereas $N_2 < N_1$ when the latter is exposed to an oxidant gas such as NO_2.

The SnO_2 parameters used in simulation [6] for both top and bottom layers are the following:
The energy gap, Eg = 3.6 ev. The effective density of states in the conduction and the valence band are Nc = 3.5e18 and Nv = 1.3e19 respectively. The electron mobility, μ = 20 $m^2.v^1.s^{-1}$. The number of dopants, $N_2 = N_1$ = 1e18 when the sensor is exposed to air and N_2 = 1.5e18 when it is exposed to an oxidant gas. The top layer thickness in the 3 examples above is about 10 nm, which represents the surface of the SnO_2 film accessible to the gas. The overall thickness of the entire sample (bottom and top layers) has a value e = 25, 45 and 100 nm.
The used models are the distribution of Fermi-Dirac and the recombination of Shockley Read Hall statistics [7]. These are built-in models in SILVACO software's. We hence obtain the I-V characteristics, hence the sensor resistance. The latter is exposed to an oxidant gas such as NO_2.

2.2 Material Deposition

Undoped-SnO_2 thin films are deposited at room temperature on SiO_2/Si substrates via sputtering of a 4' SnO_2 target in an Alliance Concept RF magnetron sputtering system (AC450). Therefore, sputtering power, deposition pressure of the chamber, and annealing temperature were investigated and optimized. The optimal deposition parameters are: Sputtering power, ω = 300 W; Deposition pressure, $P = 5 \times 10^{-3}$ Pa; Films thickness, e = 25, 45 and 100 nm respectively. All the samples were then annealed for 10 min under nitrogen by rapid thermal annealing process at 450°C.

2.3 Material Characterisation

The structures of the prepared samples are investigated using X-ray diffraction XRD (Smart Lab Rigaku, Cu $K_{\alpha 1}$ radiation, λ =1.5406 Å). The morphology of the surface is studied using Atomic Force Microscopy, AFM. The chemical composition of our samples (surface + bulk) is carried out via X-ray photoelectron spectroscopy (XPS), using a customized Thermo Fisher Theta 300 spectrometer, interfaced to a specific loading interface from Pfeiffer Vacuum. The bulk chemical composition is analysed in situ in the XPS chamber by etching the sample using an Ar+ ion beam having an etching rate of approximately 1.85 nm/min.

2.4 Sensor fabrication

The sensor is manufactured by lithographic technique. The electrodes are deposited by evaporating Ti (5 nm) /Pt (40 nm) on SiO_2 (300 nm) /Si. Figure 2 shows the different geometries of the electrodes for gas sensing measurements. SnO_2 sensing films were then deposited on the inter-digitated electrodes, forming the gas sensor device (Red zone in figure 2).

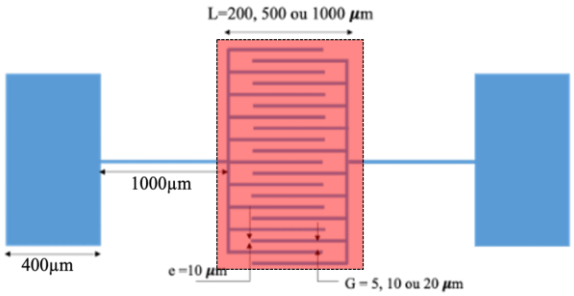

Figure 2: Device electrodes geometry (blue), and SnO_2 zone (red).

2.5 Gas sensing measurements

A testing chamber with a total volume of around 1.6 L is used to study the detection conditions. The target gas (NO_2) is delivered to the chamber via a gas system. Mass flow regulators are used to dilute the analytes in order to study the effect of the gas concentration on the response of the sensor. This dilution system allows the generation of low concentrations, ranging between few tens of ppb to 3 ppm. Sensing measurements are carried out via monitoring the electrical resistance of the sensor in real time using a Keithley 2450 source meter. The sensor is deposed on a heating substrate in order to control the temperature of the former.

3 Results and discussion

3.1 Simulation

Figure 3 shows the simulation result. The response r of the simulated sensor when exposed to the gas is given by:

$$r = \frac{R_2 - R_1}{R_2} \times 100 \qquad (1)$$

such that,

R_1: resistance of the sensor when exposed to an oxidant gas;
R_2: resistance of the sensor when exposed to the air.

On one hand, the simulation results do not show any major effects when measuring the response as function of the gap. More precisely, the response of the 25 nm thick SnO_2 only barely changes from 20% with a gap of 5 nm into roughly 19% for a gap of 10 nm. Clearly, the value of the response stays close to 19% for a gap of 20 nm. Similarly, the response of 100 nm thick SnO_2 remains around 5% as function of the gap. However, the response of the 45 nm thick SnO_2 has produced different outcomes, by changing from 11% with a gap of 5 nm into 16% for a gap of 20 nm. The reason behind such behavior is still unknown, since the two other sensors do not show the same behavior, nevertheless, it is important to note that the gap effect was not evaluated experimentally.

On the other hand, the simulation results show that SnO_2 film thickness have an effect on the sensor response. For example, the response of 25 nm thick SnO_2 is 20%, which decreases significantly to 10% for a sensor thickness of 45 nm. Similarly, the response drops to 5% for a thickness of 100 nm.
Following the above study, we conclude that an optimal sensor must have a sensing film thickness that rivals the electrodes thickness.

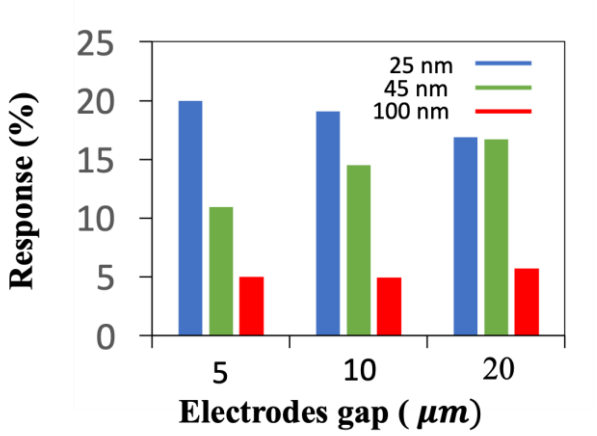

Figure 3: Response of the simulated sensors as function of the gap and the SnO_2 thickness.

3.1 Material characteristics

The microstructure of the sensing surface affects the sensitivity of the sensor such as the SnO_2 grain size. Hence, the characteristics of the deposed SnO_2 films are examined, and the results are presented below.

Phase identification

The X-ray diffraction pattern of the 100 nm thick annealed SnO_2 film is presented in figure 4. This XRD pattern shows a cassiterite structure. The SnO_2 peaks (110), (200) (211) are being indexed as shown in the figure below. Such pattern signals the formation of SnO_2 crystallites which is crucial for sensing applications. Our SnO_2 films are polycrystalline.

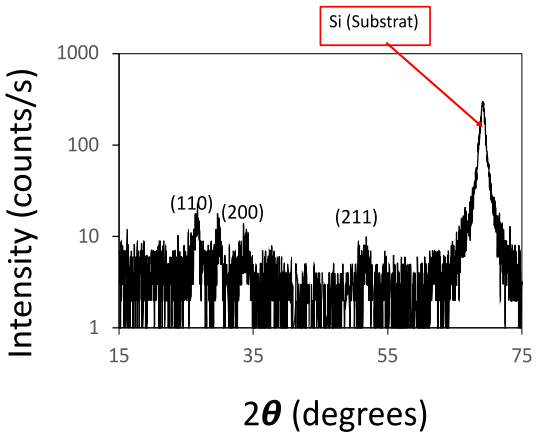

Figure 4: XRD diffraction pattern of the 100 nm undoped-SnO_2.

Morphology observation

Figure 5 presents AFM images of the surface morphology of the SnO_2 films having 25, 45 and 100 nm thickness respectively. These images are obtained using tapping-mode AFM. The size of each image is 2μm × 2μm. The below images show that the three films have a granular structure. These films differ in terms of their surface roughness along with the size of their grains. While increasing the film thickness, the grain size increases, leading to an increase of the roughness of the surface. The AFM images show the smallest grains size for the 25 nm thick SnO_2, when compared to the 45nm and 100 nm thick SnO_2. More precisely, the average size of the former film (25 nm) is 10-15 nm, whereas the average size of the latter films (45 and 100 nm) happens to be 15-25 nm and 25-35 nm respectively. On the other hand, the surface roughness, which is determined by calculating the root mean square RMS, which takes a value of 0.823 nm for the case of 25 nm, while taking a value of 1.42 nm for the 45 nm and 3.09 nm for the 100 nm thick SnO_2.

Stoichiometry

In order to study the chemical composition of our SnO_2 films, in particularly the ratio O/Sn, three SnO_2 samples, which have 100 nm thickness were deposited by sputtering. Two of these samples were annealed at 450°C using rapid thermal annealing (RTA) for 10 minutes: one is annealed in an N_2 environment, while the second one is annealed in a N_2+O_2 environment. Furthermore, the third sample is annealed at 450°C in air inside a tubular oven for 30 min.

The XPS analyses were performed for etched samples under Ar. Figure 6 shows that our films are rich in oxygen at the surface with the ratio O/Sn = 2.2 while taking a value of 1.8 in the bulk.

Such high ratio at the surface is probably either due to the long-time sample storage in the air, and / or due to the oxygen atoms being linked to the carbon atoms contamination on the surface.

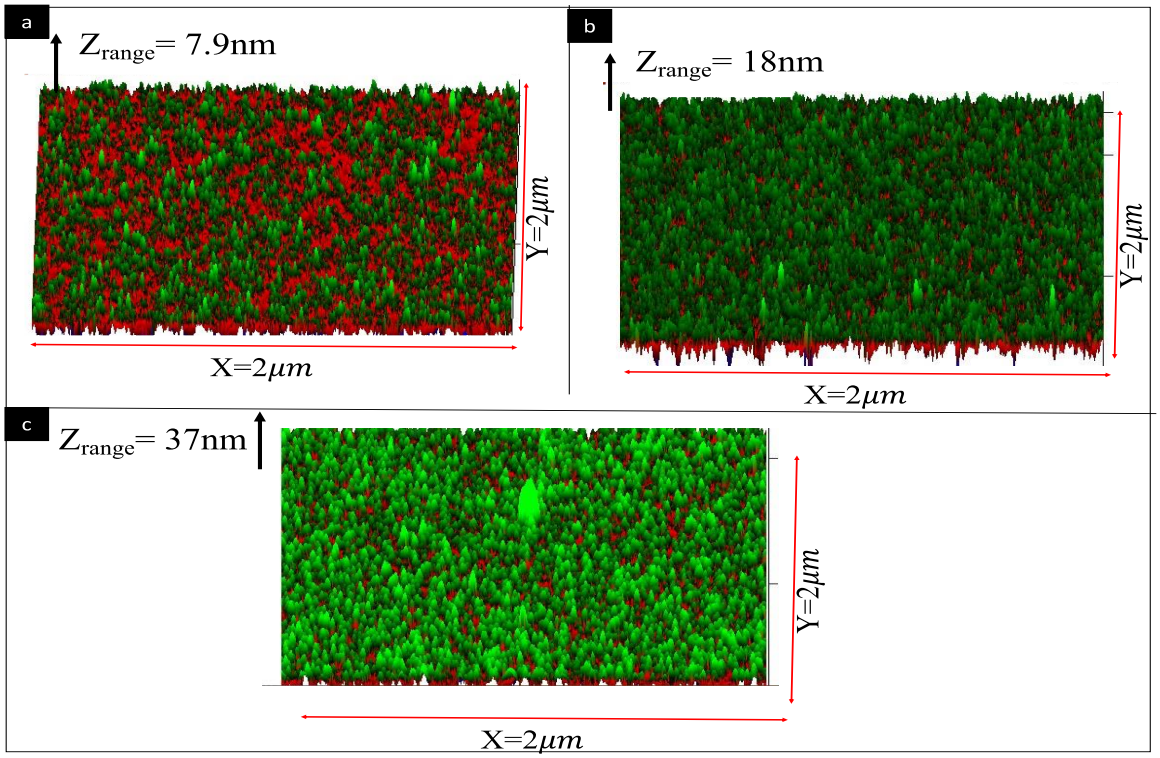

Figure 5: 3d AFM images of SnO2 films of varying thickness: a) 25 nm, b) 45 nm and c) 100 nm.

Moreover, this study has shown that the annealing conditions have no effect on the chemical composition of SnO_2.

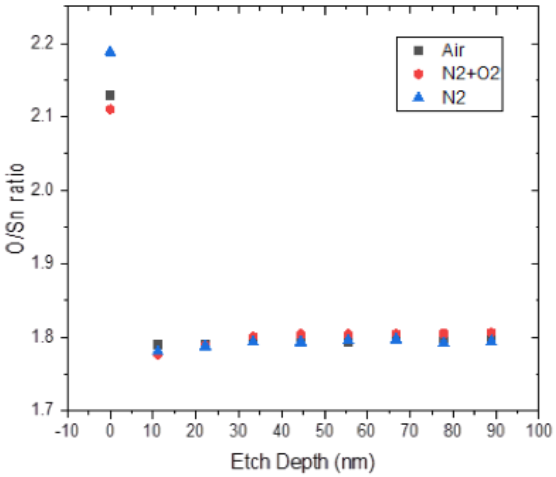

Figure 6: O/Sn ratio of 100 nm undoped SnO_2 samples as a function of etching depth. The sample are annealed in different environment (N_2, Air, N_2+O_2).

3.2 Sensing performance

In order to measure the response of our sensors, a bias of 0.05V has been applied on the electrodes. The electrical resistance is then recorded while the device is exposed to cycles of NO_2 and dry air. It is clearly demonstrated that the relative humidity influences the surface conductivity, as shown in [8]. Water molecules can enhance the sensor response toward gases. In their paper, [4]. Kiruba Mangalam Subramaniam and al. added 10% of humidity in order to detect NO_2.

The sensors in this study show low electrical resistance e. For example, the 45 nm thick-SnO_2 has a resistance of 12 kΩ in dry air at 50°C, 3.5 kΩ at 100°C, 2.6 kΩ at 150°C and 1.4 kΩ at 200°C.The latter measurements shows a better response as compared with the sensors with 25 nm and 100 nm-thick SnO_2. Figure 7 shows the real time response, r, (as defined in equation 2) for the 45 nm-thick SnO_2 sensor for multiple cycles of 3 ppm NO_2 - dry air at different working temperatures.

$$r = \frac{R_{GAS} - R_{AIR}}{R_{AIR}} \times 100 \qquad (2)$$

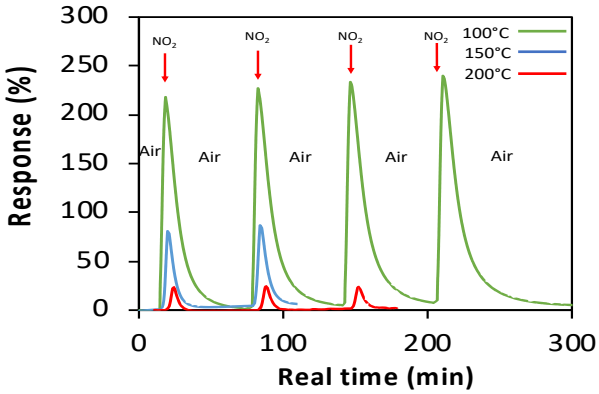

Figure 7: Response of 45 nm thick SnO_2 Sensor for 3 ppm NO_2 in real time, cycles of 4 - 60 min of 3 ppm of NO_2 - Dry air, for different working temperature.

The sensor shows the highest and the fastest gas sensing response, about 250 % towards 3 ppm of NO_2 at 100°C, in 3.4 min. At 150°C, the response is reduced to 120%, displaying a marginal slower response of 3.7 min. At 200°C, the response has dropped significantly to 25%, showing a slower response around 4.4 min. However, while increasing the temperature, the recovery time decreases, indicating that the NO_2 desorbs faster at higher temperatures. NO_2 molecules take 26.7 min to desorb at 100°C, 11.8 min at 150°C and 7.8 min at 200°C. The response r, the response time and the recovery time are given in table 1.

Moreover, the response and recovery time are affected by the chamber dimensions. More tests will be held in a smaller chamber given that the present chamber is comparably big - it has a diameter and height of 16 and 8 cm, respectively.

	r(%) ±2%	$t_{response}$ (min) ±0.1 min	$t_{recovery}$ (min) ±0.1 min
100°C	234	3.4	26.7
150°C	125	3.7	11.8
200°C	25	4.4	7.8

Table 1: The response r, response time and the recovery time.

Figure 8 displays the sensor response for different NO_2 concentrations, which exhibit a perfectly linear relationship within an accuracy of 1%. This linear behavior can be used to evaluate the sensitivity and the limit of detection (LOD) of the sensor. According to these results, the LOD of our sensor is a bit lower than 0.25 ppm.

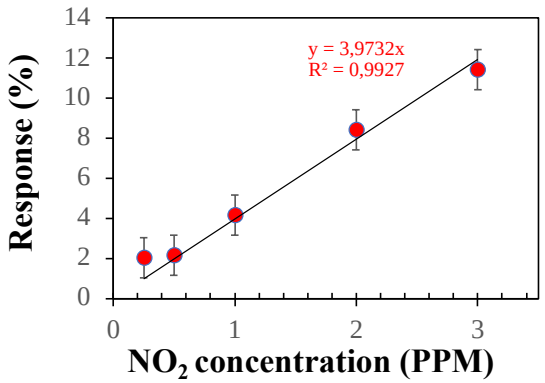

Figure 8: Relationship between the 45 nm thick SnO_2 sensor and NO_2 concentration.

At 50°C, the sensor shows a small and reproducible response of 1% (figure 9). However, the NO_2 molecules can't desorb for such a low temperature.

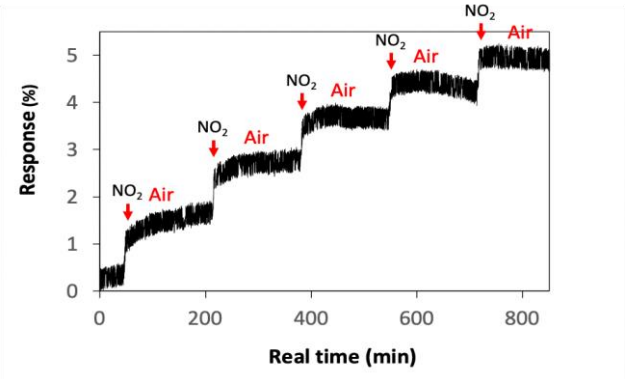

Figure 9: Response of 45 nm thick SnO_2 sensor for 3 ppm NO_2 in real time, cycles of 4- 120 min of 3 ppm NO_2 - Dry air at 50°C.

4 DISCUSSION

In this study, we have shown that lowering the operating temperature of NO_2 sensors using undopped-SnO_2 is possible. In this section, we intend to compare our results to others found in the literature.

D. L. Kamble synthesized NO_2 gas sensor of nanocrystalline SnO_2 using different spray solution concentrations [10]. The optimal operating temperature for detecting 40 ppm of NO_2 using this sensor is reported to be 150 °C.

G. D. Khuspe synthesized SnO_2 nanostructure via sol-gel spin coating technique [11]. His sensor demonstrated the highest response of 19% towards 100 ppm NO_2 at an operating temperature of 200 °C. When compared to the above studies, it is clear to deduce that our undoped-SnO_2 is shown to be more sensitive which operates at lower temperature of 100°C. Moreover, it reacts with NO_2 at 50°C.

The reason why our sensor reacts at lower temperatures could be attributed to multiple reasons. The most important ones in our case are the SnO_2 microstructure and the chemical composition.

On the other hand, the sensor geometry has also its role in the gas detection. this is clearly seen when the 100 nm thick SnO_2 did not show any response. Such behavior does not mean that the SnO_2 film didn't react with NO_2, but the geometry of the SnO_2 sensor was not accurately chosen.

5 SUMMARY

In this work, we have demonstrated low temperature (100°C) gas sensing properties with a detection of 3 ppm - NO_2 using undoped-SnO_2 sensor deposited using conventional RF-sputtering. Moreover, the SnO_2 sensing layer shows a response to NO_2 at 50°C. Nevertheless, NO_2 molecules can not be desorbed at this temperature. Further investigations are required to improve the sensing operation at 50°C.

ACKNOWLEDGEMENTS

This work has received a partially funding from IPCEI-Nano2022 and was partly supported by the French RENATECH network through the PTA technological platforms in Grenoble and by the EquipEx IMPACT program, managed by the ANR French agency (ANR-10-EQPX-33). A Part of this work was also realised at NANOLYON Platform for material deposition and characterisation. Gas sensing benches from IM2NP laboratory have been used for NO_2 sensor characterizations.

REFERENCES

[1] Environmental Protection Agency (EPA) Nitrogen Dioxide (NO_2) Pollution, https://www.epa.gov/no2-pollution [Last updated on June 7, 2021].

[2] Hayat Hasan, "The State-of-the-Art of Sensors and Environmental Monitoring Technologies in Buildings" Sensors2019, 19, 3648; (2019), https://doi:10.3390/s19173648.

[3] Yong Wang, "Sputtered SnO_2: NiO thin films on self-assembled Au nanoparticle arrays for MEMS compatible NO2 gas sensors,"Sensors and Actuators B: Chemical Volume 278, 2019, https://doi.org/10.1016/j.snb.2018.09.074.

[4] Kiruba Mangalam Subramaniam, "Sputter deposited p-NiO/n-SnO_2 porous thin film heterojunction based NO2 sensor with high selectivity and fast response" Sensors and Actuators B: Chemical, 2020, https://doi.org/10.1016/j.snb.2020.127830

[5] N. Barsan, "Metal oxide-based gas sensor research: How to?," *Sens. Actuators B Chem.* , vol. 121, p. 18–35, 2007. https://doi.org/10.1016/j.snb.2006.09.047.

[6] Kadiyam Rajshekar, "A Comprehensive Density-of-States Model for Oxide Semiconductor Thin Film Transistors", 2021, research square. https://doi.org/10.1007/s10825-021-01783-8.

[7] W. Shockley, "Statistics of the Recombinations of Holes and Electrons",Phys. Rev. 87 (1952), pp. 835-842.
https://doi.org/10.1103/PhysRev.87.835.

[8] J.F.McAleer Tin Dioxide Gas sensors: Part 1. *JChemSoc, Faraday Trans* 1987, 1:1323-1346. Journal Article.

[9] A. A. Haidry , " Investigating the influence of Al-doping and background humidity on NO_2 sensing characteristics of magnetron-sputtered SnO_2 sensors", Journal of sensors and Sensor Systems, 4, 271–280, 2015, doi:10.5194/jsss-4-271-2015.

[10] Kamble DL, Harale NS, Patil VL, Patil PS, Kadam LD. Characterization and NO2 gas sensing properties of spray pyrolyzed SnO2 thin films. J Anal Appl Pyrolysis. 2017; 127(2): 38–46.

[11] Khuspe GD, Navale ST, Bandgar DK, Sakhare RD, Chougule MA, Patil VB. SnO2 nanoparticles-modified polyaniline films as highly selective, sensitive, reproducible and stable ammonia sensors. Electron Mater Lett. 2014; 10(1): 191–7.